



## Experimental realization of all-dielectric composite cubes/rods left-handed metamaterial

Jun Wang, Zhuo Xu, Zhenhua Yu, Xiaoyong Wei, Yiming Yang et al.

Citation: *J. Appl. Phys.* **109**, 084918 (2011); doi: 10.1063/1.3575326

View online: <http://dx.doi.org/10.1063/1.3575326>

View Table of Contents: <http://jap.aip.org/resource/1/JAPIAU/v109/i8>

Published by the [AIP Publishing LLC](#).

---

### Additional information on *J. Appl. Phys.*

Journal Homepage: <http://jap.aip.org/>

Journal Information: [http://jap.aip.org/about/about\\_the\\_journal](http://jap.aip.org/about/about_the_journal)

Top downloads: [http://jap.aip.org/features/most\\_downloaded](http://jap.aip.org/features/most_downloaded)

Information for Authors: <http://jap.aip.org/authors>

## ADVERTISEMENT



**Running in Circles Looking  
for the Best Science Job?**

Search hundreds of exciting  
new jobs each month!

<http://careers.physicstoday.org/jobs>

physicstodayJOBS



# Experimental realization of all-dielectric composite cubes/rods left-handed metamaterial

Jun Wang,<sup>1,2,a)</sup> Zhuo Xu,<sup>1,2</sup> Zhenhua Yu,<sup>1,2</sup> Xiaoyong Wei,<sup>1,2</sup> Yiming Yang,<sup>3</sup> Jiafu Wang,<sup>3</sup> and Shaobo Qu<sup>1,3</sup>

<sup>1</sup>Electronic Materials Research Laboratory, Key Laboratory of the Ministry of Education, Xi'an Jiaotong University, Xi'an 710049, People's Republic of China

<sup>2</sup>International Center for Dielectric Research, Xi'an Jiaotong University, Xi'an 710049, People's Republic of China

<sup>3</sup>College of Science, Air Force Engineering University, Xi'an 710051, People's Republic of China

(Received 22 December 2010; accepted 4 March 2011; published online 28 April 2011)

We present a novel all-dielectric left-handed metamaterial (LHM) in the X-band microwave regime. The LHM is formed by cubes and square rods, which are made of microwave ceramic with high permittivity and low loss. Both Mie theory and dielectric resonator theory are found to play important roles in generating negative effective parameters. The effective permeability is negative in the designed frequency range due to the first Mie resonance associated with the cubes, while the effective permittivity is negative below the plasma frequency owing to the second resonance mode of the square rods. The parameter retrieval method, transmission spectra method and wedge-shaped negative refraction method are used to demonstrate that the composite has a double-negative regime. Experiments are carried out to verify the designed all-dielectric LHM. The proposed method presents new ways to realize all-dielectric LHMs. © 2011 American Institute of Physics. [doi:10.1063/1.3575326]

## I. INTRODUCTION

Left-handed metamaterials (LHMs) are artificial materials that possess negative permeability and negative permittivity simultaneously. The electromagnetic properties of EM waves in LHMs are dramatically different from those in natural substances<sup>1–4</sup> LHMs may enable some exotic applications such as negative refraction,<sup>5</sup> backward wave<sup>6</sup> and inverse Doppler effect,<sup>7</sup> as well as unique applications in subwavelength imaging,<sup>8</sup> and electromagnetic cloaking,<sup>9</sup> etc.

Metal-based realizations of LHMs were proposed with various unit cell geometries including omega-shaped structures,<sup>10</sup> S-shaped structures,<sup>11</sup> fishnet structures,<sup>12</sup> fractal structures,<sup>13,14</sup> etc. However, these metallic structures are highly anisotropic. Their corresponding isotropic realizations demand three-dimensional arrangements that are quite complicated in fabrication. In addition, due to their complicated geometries and enhanced conductive losses with increasing the frequency, they cannot be scaled up to infrared and optical frequencies.<sup>15</sup>

As an alternative, composites composed of high dielectric inclusions can overcome the mentioned limitations by using simple isotropic structures at high frequencies. Two- or three-dimensional regular or random arrays of high dielectric rods,<sup>16–18</sup> spheres,<sup>19,20</sup> and cubes<sup>21</sup> were fabricated and examined. Holloway<sup>19</sup> proposed a method of realizing electric dipoles and magnetic dipoles by using magnetodielectric spherical particles. Vendik<sup>20</sup> proposed a composite material consisting of two sets of spheres with different radii to realize the double-negative property. Zhao *et al.*<sup>21,22</sup> reported

that isotropic negative permeability can be realized in a three-dimensional dielectric composite consisting of an array of dielectric cubes, and they also demonstrated that the combination of dielectric cubes and metallic wires produced a left-handed transmission. Peng *et al.*<sup>16</sup> reported an observation of negative refraction with a prism of ferroelectric rods, where the second resonant mode was considered.

In this paper, we present an all-dielectric LHM in X-band. The LHM consists of a matrix of acrylonitrile butadiene styrene (ABS) plastic, with cubes and square rods regularly embedded within it. The embedded inclusions, cubes and square rods, are made of microwave ceramics (BST), which possess high permittivity and low loss. The effective permeability is negative in some frequency range due to a Mie resonance associated with the cubes, while the effective permittivity is negative below the plasma frequency of the square rods. The dimensions of the BST cubes and square rods are selected, in order to obtain negative refractive index in X-band. The main advantages of this design are the intrinsic low losses of all-dielectric inclusions and easy realization of simultaneous  $\epsilon_{\text{eff}} < 0$  and  $\mu_{\text{eff}} < 0$ . Meanwhile, the regular arrangement sample can be easily fabricated.

This paper is organized as follows: Mie resonances with effective medium theory and dielectric resonator theory are introduced and discussed in Sec. II. Section III presents the simulation results of the designed LHM. The origination of negative permeability and permittivity is discussed using Mie theory and dielectric resonator theory. Field analysis method is also introduced to make a further interpretation. Then, in Sec. IV, an experiment is designed to test the validity of the simulation results. Finally, we summarize the results in Sec. V.

<sup>a)</sup>Electronic mail: wangjun563@163.com.

## II. THEORETICAL ANALYSES

In this paper, the permittivity of inclusions is much larger than that of the background matrix. That is to say, the wavelengths inside the inclusions are comparable to the dimensions of the inclusions, while the wavelengths outside the inclusions are larger than the dimensions of the inclusions. Thus, the composite can be described by the effective medium theory. The related parameters could be calculated and explained by using the framework of Mie theory<sup>23</sup> and dielectric resonator theory.

### A. Mie theory of high dielectric spheres

Consider dielectric spheres of radius  $r_0$  and relative permittivity  $\varepsilon_2$  embedded in a host medium with a relative permittivity  $\varepsilon_1$ . Let  $v$  denote the volume filling fraction occupied by the spheres in the composite and  $x$  represents the sphere size parameter,  $x_1 \equiv k_1 r = \sqrt{\varepsilon_1} 2\pi f r / c$ ,  $x_2 \equiv k_2 r = \sqrt{\varepsilon_2} 2\pi f r / c$ . According to the extended Maxwell–Garnett theory,<sup>24,25</sup> provided that  $x_1 \ll 1$  (the so-called quasistatic limit), the effective permittivity and permeability of the composites are given by

$$\varepsilon_{\text{eff}} = \varepsilon_1 \frac{x_1^3 + 3ivT_1^E}{x_1^3 - \frac{3}{2}ivT_1^E}, \quad (1)$$

$$\mu_{\text{eff}} = \mu_1 \frac{x_1^3 + 3ivT_1^H}{x_1^3 - \frac{3}{2}ivT_1^H}, \quad (2)$$

where  $T_1^E$  and  $T_1^H$  are the electric-dipole components and the magnetic-dipole components of the scattering  $T$ -matrix of a single sphere, respectively. Explicit expressions of  $T_1^E$  and  $T_1^H$  are given by:

$$T_1^E = \frac{\varepsilon_2 J_1(x_2)[x_1 J_1(x_1)]' - \varepsilon_1 J_1(x_1)[x_2 J_1(x_2)]'}{\varepsilon_2 H_1^{(2)}(x_1)[x_2 J_1(x_2)]' - \varepsilon_2 J_1(x_2)[x_1 H_1^{(2)}(x_1)]'}, \quad (3)$$

$$T_1^H = \frac{J_1(x_2)[x_1 J_1(x_1)]' - J_1(x_1)[x_2 J_1(x_2)]'}{H_1^{(2)}(x_1)[x_2 J_1(x_2)]' - J_1(x_2)[x_1 H_1^{(2)}(x_1)]'}, \quad (4)$$

where  $J_1(x)$  is the spherical Bessel function and  $H_1^{(2)}(x)$  is the spherical Hankel function of the second kind, which can be written as a form of trigonometric functions, that is,  $J_1(x) = (\sin x - x \cos x)/x^2$  and  $H_1^{(2)}(x) = (i/x^2 - 1/x)e^{-ix}$ . In the quasistatic limit  $x_1$  approaches zero, it can be found that  $J_1(x) \rightarrow (1/3)x_1$ ,  $J_1'(x_1) \rightarrow 1/3$ ,  $H_1^{(2)}(x_1) \rightarrow i/x_1^2$  and  $H_1^{(2)'}(x_1) \rightarrow -2i/x_1^3$ . Define  $x_2 \equiv \theta$  and  $F(\theta) = [2(\sin \theta - \theta \cos \theta)]/[(\theta^2 - 1) \sin \theta + \theta \cos \theta]$ , the coefficient for the spherical harmonics in the first Mie resonance mode can be reduced to

$$T_1^H = i \frac{2x_1^3}{3} \frac{1 - F(\theta)}{2 + F(\theta)} \quad (5)$$

By combining Eqs. (2) and (5), the effective permeability of the composites can be written as

$$\mu_{\text{eff}} = 1 + \frac{3v}{\frac{F(\theta) + 2}{F(\theta) - 1} - v}. \quad (6)$$

Equation (6) shows that the effective permeability can be negative in a proper frequency range in case of suitable dimensions.

There is only one dielectric sphere in free space when the volume fraction ( $v$ ) approaches zero. Under this condition, the magnetic resonance frequency is equal to the first-order TE mode resonant frequency given by Mie scattering theory for a single dielectric sphere. If dielectric constant of the sphere resonator is 90 and the radius 1.5 mm, the first order free resonant frequency is calculated to be  $f = 10.54$  GHz.

### B. Dielectric resonator theory of high dielectric spheres

The origination of negative permeability can also be interpreted in the view of dielectric resonator theory, being consistent with Mie theory. The first resonant mode of the dielectric sphere resonator is TE<sub>101</sub> mode. The characteristic equation can be written as

$$\frac{[x_2 J_1(x_2)]'}{\mu_2 J_1(x_2)} = \frac{[x_1 H_1^{(2)}(x_1)]'}{\mu_1 H_1^{(2)}(x_1)}. \quad (7)$$

By solving this equation, we have  $f = c/2r\sqrt{\varepsilon_r}$ . As the permittivity of the sphere resonator is 90 and the radius 1.5 mm, the resonant frequency of TE<sub>101</sub> mode is  $f = 10.54$  GHz. It is equal to the first order free resonant frequency of TE mode given by Mie scattering theory. Thus, we can conclude that both Mie theory and dielectric resonator theory play important roles in generating negative effective parameters.

### C. Dielectric resonator theory of high dielectric cubes and square rods

Rectangular dielectric resonators (RDR) rather than sphere ones are studied in present work because they can be easily fabricated. The resonant modes of rectangular dielectric resonators are mainly TE <sub>$mn(s+\delta)$</sub>  and TM <sub>$mn(s+\delta)$</sub> . The first modes are TE<sub>11 $\delta$</sub>  and TM<sub>11 $\delta$</sub> , respectively.

The frequencies of TE <sub>$mn(s+\delta)$</sub>  modes can be calculated using the following formulas:

$$f_0 = \frac{c}{2\pi\sqrt{\varepsilon_r}} \sqrt{\left(\frac{m\pi}{a}\right)^2 + \left(\frac{n\pi}{b}\right)^2 + \left(\frac{(s+\delta)\pi}{l}\right)^2}, \quad (8)$$

$$k_z l = s\pi + 2tg^{-1}\left(\frac{\alpha_z}{k_z}\right), \quad (9)$$

$$k_z^2 + \alpha_z^2 = (\varepsilon_r - 1)k_0^2, \quad (10)$$

$$k_0 = 2\pi f_0 / c, \quad (11)$$

where  $a$ ,  $b$  and  $l$  are dimensions of the RDR,  $\varepsilon_r$  the relative permittivity of the RDR. For a dielectric cube with  $a = b = l = 2.4$  mm,  $\varepsilon_r = 100$ , the calculated frequency of TE<sub>11 $\delta$</sub>  mode is 9.69 GHz, being similar to the frequency simulated by HFSS (10.28 GHz, the relative error is 4%). For a square rod with  $a = 10.16$  mm,  $b = l = 1.5$  mm,  $\varepsilon_r = 100$ , the calculated frequency of TE<sub>11 $\delta$</sub>  mode is 11.95 GHz. By substituting  $k_z l = s\pi + 2tg^{-1}(\varepsilon_r \alpha_z / k_z)$  for Eq. (9), the frequency of TM<sub>11 $\delta$</sub>  mode is found to be 10.16 GHz.

### III. SIMULATION AND ANALYSES

The proposed LHM is based on the assumption that the cubes under the first resonant mode produce a negative permeability, while the square rods under the second resonant mode produce a broadband negative permittivity. In principle, microwave dielectric ceramics with high permittivities and low losses can be used to achieve left-handed bands by a proper design. In this paper, magnesium titanate lanthanum doped barium strontium titanate (BST-LMT) with  $\epsilon_2 \approx 100$ ,  $\tan \delta \approx 0.0016$  around 10 GHz is used as inclusions embedded in a matrix with  $\epsilon_1 = 2.67$ ,  $\tan \delta = 0.006$ . The parameter retrieval method, transmission spectra method and wedge-shaped negative refraction method are used to determine the left-handed properties.

As shown in Fig. 1, the proposed model, consisting of BST-LMT cubes and square rods, is displayed in an X-band waveguide. The model is designed and calculated by a full wave finite element method (FEM) simulator (Ansoft HFSS). The X-band waveguide with a cross-section of  $22.86 \times 10.16 \text{ mm}^2$  works in 8–12 GHz. The boundary condition of the side walls of the waveguide is set as perfect electric conductor (PEC). The mode excited in the wave port is  $\text{TE}_{10}$  mode. The simulator can give  $S$  parameters and electromagnetic field distributions with a high accuracy when the convergence condition is satisfied.

Both the  $S$  parameters and the retrieved effective electromagnetic parameters are described in Fig. 2. The medium with both cubes and square rods has a passband around

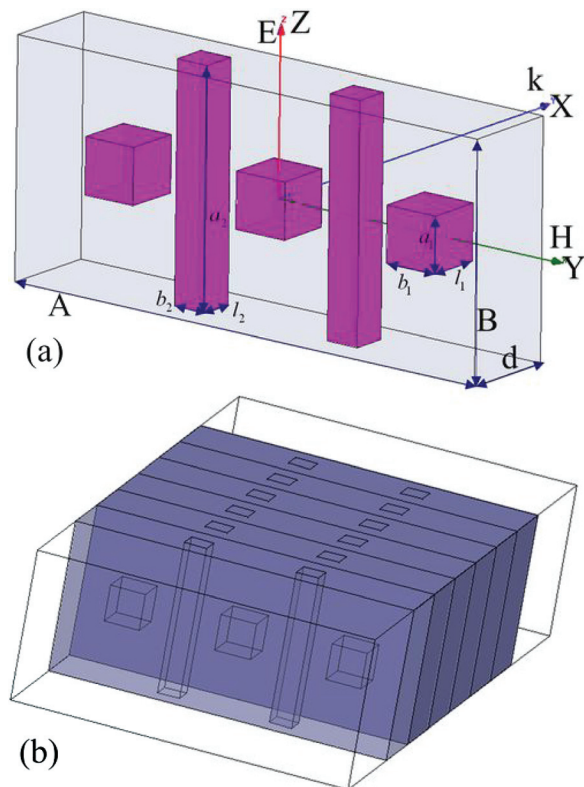


FIG. 1. (Color online) (a) Geometrical parameters of the LHM are:  $a_1 = b_1 = l_1 = 2.4 \text{ mm}$ ,  $a_2 = 10.16 \text{ mm}$ ,  $b_2 = l_2 = 1.5 \text{ mm}$ ,  $A = 22.86 \text{ mm}$ ,  $B = 10.16 \text{ mm}$ ,  $d = 4.24 \text{ mm}$ . (b) LHM with six layers is displayed in an X-band rectangular waveguide working in the  $\text{TE}_{10}$  mode.

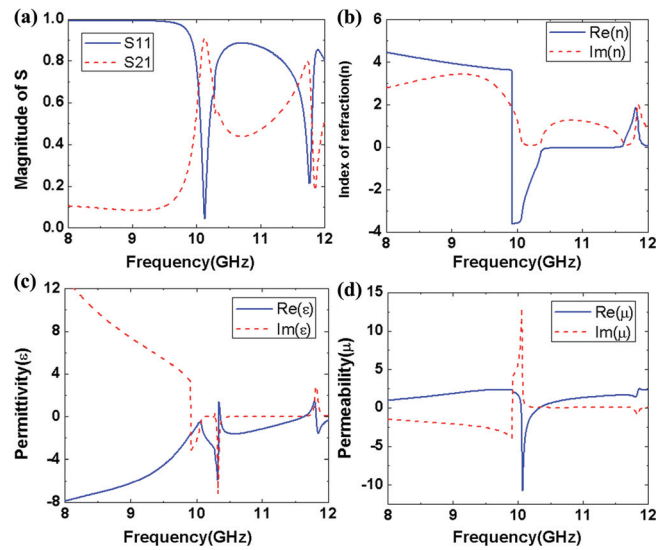


FIG. 2. (Color online) The simulated transmission spectra and effective parameters of the proposed model. (a) Magnitude of the simulated  $S$  parameters, (b) retrieved refractive index, (c) effective permittivity, (d) effective permeability.

10 GHz. The retrieved parameters demonstrate that this passband is left-handed due to simultaneous appearances of negative refractive index, negative effective permittivity and negative permeability.

The transmission spectra for the LHM and individual inclusions are given and compared in Fig. 3. Left-handed band can be determined intuitively by comparing the transmission spectra. The retrieved parameters for individual cubes and square rods reveal the origination of negative permittivity and negative permeability.

From Fig. 3(a), it can be found that there is a stop band around 10 GHz for cube-only and rod-only cases. The

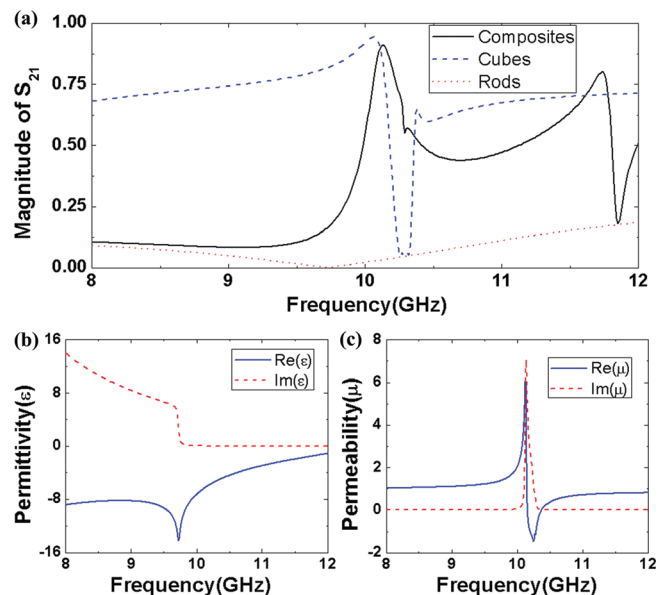


FIG. 3. (Color online) Comparison of transmission spectra and effective parameters. (a) Transmission spectra for the composites with both cubes and square rods (solid line), only cubes (dashed line) and only square rods (dotted line). (b) Retrieved permittivity of the composites with only square rods. (c) Retrieved permeability of the composites with only cubes.

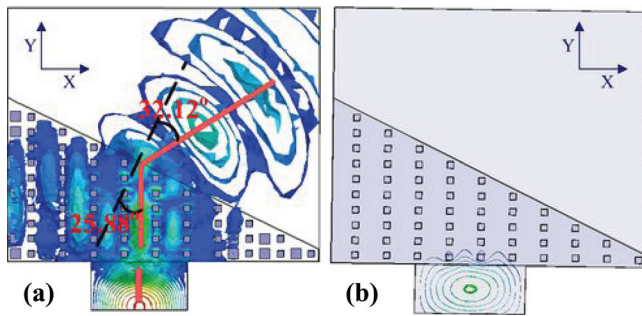


FIG. 4. (Color online) Transmission characteristics of the wedge-shaped composites. (a) Wedge-shaped composite with cubes and square rods inside demonstrate negative refraction and negative phase velocity at 10.3 GHz. (b) Wedge-shaped composite with square rods inside demonstrate a stop band at 10.3 GHz.

effective permittivity for square rod only is negative in the range of 9.8–12 GHz. The electric response of rod-only is similar to that of metal wires (Drude model). Thus, it give rise to a super wide stop band [Fig. 3(b)]. The composite with only cubes inside has a magnetic resonance nearby 10 GHz. The effective permeability is negative in part of the antiresonance frequencies range, leading to a narrow stop band, as shown in Fig. 3(c). To realize a left-handed passband, two stop bands are combined together by using the composite with both cubes and square rods inside.

We further prove that the proposed medium has negative refraction by simulating the electric field distribution of a wedge-shaped composite. As shown in Fig. 4(a), the wedge-shaped sample is made of left-handed medium consisting of high dielectric cubes and square rods. It contains 10 unit cells along the direction of the incident wave and is placed in a parallel-plate waveguide. The electric field distribution at 10.3 GHz is obtained by simulation. The EM wave, which is incident from the bottom wave port, has a positive phase velocity (+y direction) in vacuum while a negative phase velocity (−y direction) in the LHM medium. The image clearly shows that the wave has a negative refraction at 10.3 GHz. By measuring the refractive angles and applying Snell's law, the refractive index is calculated to be  $-1.22$ , which is consistent with the retrieved one. Figure 4(b) shows a wedge-shaped medium consisting of square rods. This medium has a stop band nearby 10.3 GHz. Further investigations demonstrate that this medium has a negative permittivity.

For a square rod with  $\epsilon = 100$ ,  $a = 10.16$  mm (along the electric vector),  $b = l = 1.5$  mm, the calculated frequencies for  $TM_{11\delta}$  mode and  $TE_{11\delta}$  mode are 10.16 and 11.95 GHz, respectively. Figure 5 shows that the square rod produces a wideband plasma resonant behavior, which is as same as the electric response of a metallic rod array. This kind of broadband plasma resonant behavior is derived from two contradictory displacement currents generated by modulated  $TE_{11\delta}$  mode. The  $TE_{11\delta}$  mode is modulated by a good contact between the square rods and the inner walls of the waveguide. The permittivity is negative with an extreme low loss in 10.16–11.95 GHz.

As mentioned at the beginning of this section, negative permeability is derived from the first resonant mode of high permittivity cubes. For a cube with  $\epsilon = 100$ ,  $a = b = l = 2.4$

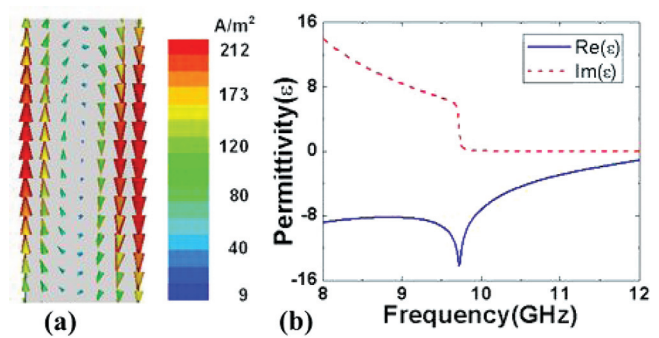


FIG. 5. (Color online) Displacement currents and retrieved parameters of modulated  $TE_{11\delta}$  mode. (a) The distribution of displacement currents of the square rods at 10.12 GHz. (b) Retrieved effective permittivity of the square rods.

mm, the calculated  $\delta$  of  $TE_{11\delta}$  mode is 0.7021 and the frequency 9.87 GHz. The frequency (9.87 GHz) given by dielectric resonator theory has a relative error of 4% to the first resonant frequency (10.28 GHz) by HFSS simulation. We can therefore infer that the first resonant mode is  $TE_{11\delta}$  mode. The field distribution in Fig. 6 proves that the resonant mode is indeed  $TE_{11\delta}$  mode and reveals how the negative permeability comes out.

As expected from Mie resonance theory, the first order Mie resonance occurs when the frequency of the incident wave is equal to the frequency of the first order TE partial wave of the cube. The resonant mode is  $TE_{11\delta}$  mode. Under this mode, an annular electric field is generated inside the cube. The electric field induces a strong annular displacement current. Meanwhile, the annular displacement current inspires a strong magnetic field, which makes the dielectric cube equivalent to a magnetic dipole in the far field region. Then, the negative permeability can be achieved near the anti-resonance region of a magnetic dipole resonance.

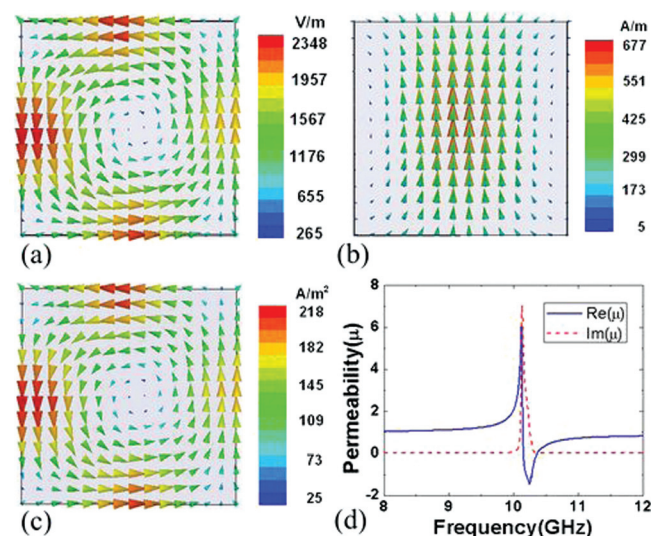


FIG. 6. (Color online) Simulated field distribution in the cube resonator. TE wave propagate along the y axis, with the magnetic field and electric field polarized along the x and z axis, respectively. (a) Electric field distribution in the y-o-z plane. (b) Magnetic field distribution in the x-o-y plane. (c) Displacement current distribution in the y-o-z plane. (d) Retrieved effective permeability of the cube.

#### IV. EXPERIMENTAL VERIFICATION

A dielectric ceramic material,  $\text{Ba}_{0.6}\text{Sr}_{0.4}\text{TiO}_3\text{-La}(\text{Mg}_{0.5}\text{Ti}_{0.5})\text{O}_3$ , was used to fabricate the dielectric inclusions for its high permittivity and low loss at microwave frequencies.  $\text{Ba}_{0.6}\text{Sr}_{0.4}\text{TiO}_3$  (BST) and  $\text{La}(\text{Mg}_{0.5}\text{Ti}_{0.5})\text{O}_3$  (LMT) were mixed in a proper proportion to decrease the loss. The BST/LMT powder was synthesized by a conventional solid state ceramics process. The analytically pure  $\text{BaCO}_3$ ,  $\text{SrCO}_3$ ,  $\text{TiO}_2$ ,  $\text{MgO}$  and  $\text{La}_2\text{O}_3$  were mixed in stoichiometric proportion to prepare  $\text{Ba}_{0.6}\text{SrTiO}_3$  and  $\text{La}(\text{Mg}_{0.5}\text{Ti}_{0.5})\text{O}_3$ , respectively. Then they were ball-milled for 12 h with ethanol and ZrO balls as the milling medium. The mixed BST powder and the mixed LMT powder were calcined at 1200 and 1400 °C for 2 h, respectively, after drying and sieving to form the crystalline powder. BST and LMT were mixed by a proportion of 0.7BST + 0.3LMT. After this, a 5% PVA solution was added for granulation. After 3 h sintering at 500 °C for latex drainage, the ceramic was obtained by sintering at 1500 °C in the air for 6 h. The microwave scattering parameters were measured in a  $\text{TE}_{01\delta}$  mode cylindrical cavity by an HP8720ES network analyzer. The parameters of the prepared cylindrical ceramic with a height 5.48 mm and a diameter 5.18 mm were measured and calculated as follows: the resonant frequency  $f_0$  is 5.085 GHz, quality factor  $Q$  632, relative permittivity  $\epsilon$  103, and loss  $\tan \delta$  0.0016.

It can be seen that the prepared ceramics totally meet the needs of fabricating an all-dielectric LHM. Then, the ceramics were cut into cubes and square rods with the dimensions  $2.4 \times 2.4 \times 2.4 \text{ mm}^3$  and  $10.16 \times 1.5 \times 1.5 \text{ mm}^3$ , respectively. The matrix is made of ABS plastic with  $\epsilon_1 = 2.67$  and  $\tan \delta = 0.006$ . The LHM composite and the measurement system are shown in Fig. 7.

The waveguide-based measurement system is composed of an X-band rectangular waveguide and an HP8720ES network analyzer. The fabricated sample with a cross section of  $22.86 \times 10.16 \text{ mm}^2$  and a thickness of 4.24 mm is placed in the waveguide. The measured results are plotted in Fig. 8. As shown in Fig. 8(a), there is a transmission passband around 10 GHz, being consistent with the simulated results in Fig. 2(a). The retrieved refractive index [Fig. 8(b)] is negative between 9.97 and 10.4 GHz. The effective permittivity has a wide negative band below the plasma frequency while the effective permeability is negative in 9.99–10.17 GHz. The left-handed bandwidth is restricted by the bandwidth of negative permeability regime. Thus, the way to achieve wideband permeability is meaningful for a further study in

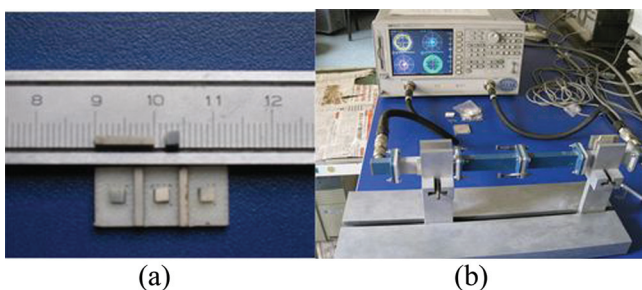


FIG. 7. (Color online) (a) The fabricated all dielectric LHM. (b) The HP8720ES analyzer based X-band rectangular waveguide testing system.

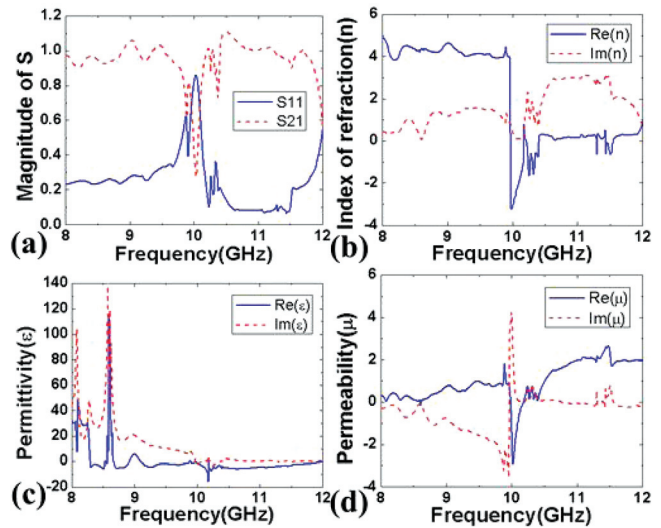


FIG. 8. (Color online) The measured transmission spectra and retrieved effective parameters of the fabricated LHM sample. (a) Magnitude of the measured  $S$  parameters, (b) retrieved refractive index, (c) effective permittivity, (d) effective permeability.

the future. The measured permittivity [Fig. 8(c)] is different from the simulated permittivity [Fig. 2(c)] below 9 GHz. This difference is mainly because the square rods are not contacted well with the side walls of the waveguide. The measured results demonstrate that the composite cube/rod all-dielectric structure can realize left-handed properties.

#### V. CONCLUSIONS

We have fabricated a novel all-dielectric left-handed metamaterial. The LHM is composed of dielectric cubes and square rods using microwave ceramic with high permittivity and low loss. The proposed LHM can be easy to scale up to infrared and optical frequencies with proper dielectric inclusions. By retrieving the effective permittivity and permeability, we demonstrate that the composite possess a double-negative regime. Negative refraction is found in the simulations of the wedge-shaped composite. The refractive index obtained by the Snell's law is in good agreement with the retrieved parameters. Furthermore, a backward wave transmitted in the wedge-shaped composite is observed through the animated electric field distribution. The origination of negative permeability and permittivity is discussed using Mie theory and dielectric resonator theory. Finally, our designed experiment proves the validity of the simulation results. The proposed method provides a way to the design of all-dielectric metamaterials with negative refractive index, negative permittivity and negative permeability simultaneously.

#### ACKNOWLEDGMENTS

This work is supported by National Basic Research Program of China (973 Program) (Grant No. 2009CB623306), International Science & Technology Cooperation Program of China (Grant No. 2010DFR50480), National Nature Science foundation of China-NSAF (Grant No. 10976022), and the National Nature Science foundation of China (Grant No. 50632030).

- <sup>1</sup>V. G. Veselago, *Sov. Phys. Usp.* **10**, 509 (1968).
- <sup>2</sup>J. B. Pendry, A. J. Holden, W. J. Stewart, and I. Youngs, *Phys. Rev. Lett.* **76**, 4773 (1996).
- <sup>3</sup>J. B. Pendry, A. J. Holden, D. J. Robbins, and W. J. Stewart, *IEEE Trans. Microwave Theory Tech.* **47**, 2075 (1999).
- <sup>4</sup>D. R. Smith, W. J. Padilla, D. C. Vier, S. C. Nemat-Nasser, and S. Schultz, *Phys. Rev. Lett.* **84**, 4184 (2000).
- <sup>5</sup>R. A. Shelby, D. R. Smith, and S. Schultz, *Science* **292**, 77 (2001).
- <sup>6</sup>D. R. Smith and N. Kroll, *Phys. Rev. Lett.* **85**, 2933 (2000).
- <sup>7</sup>N. Seddon and T. Bearpark, *Science* **302**, 1537 (2003).
- <sup>8</sup>J. B. Pendry, *Phys. Rev. Lett.* **85**, 3966 (2000).
- <sup>9</sup>J. B. Pendry, D. Schurig, and D. R. Smith, *Science* **312**, 1780 (2006).
- <sup>10</sup>J. Huangfu, L. Ran, H. Chen, X. Zhang, K. Chen, T. M. Grzegorzczak, and J. A. Kong, *Appl. Phys. Lett.* **84**, 1537 (2004).
- <sup>11</sup>H. Chen, L. Ran, J. Huangfu, X. Zhang, K. Chen, T. M. Grzegorzczak, and J. A. Kong, *Phys. Rev. E* **70**, 057605 (2004).
- <sup>12</sup>G. Dolling, C. Enkrich, M. Wegener, C. M. Soukoulis, and S. Linden, *Opt. Lett.* **31**, 1800 (2006).
- <sup>13</sup>Y. Yao and X. P. Zhao, *J. Appl. Phys.* **101**, 124904 (2007).
- <sup>14</sup>F. Miyamaru, Y. Saito, M. W. Takeda, B. Hou, L. Liu, W. Wen, and P. Sheng, *Phys. Rev. B* **77**, 045124 (2008).
- <sup>15</sup>J. Zhou, T. Koschny, M. Kafesaki, E. N. Economou, J. B. Pendry, and C. M. Soukoulis, *Phys. Rev. Lett.* **95**, 223902 (2005).
- <sup>16</sup>L. Peng, L. Ran, H. Chen, H. Zhang, J. A. Kong, and T. M. Grzegorzczak, *Phys. Rev. Lett.* **98**, 157403 (2007).
- <sup>17</sup>K. Vynck, D. Felbacq, E. Centeno, A. I. Cabuz, D. Cassagne, and B. Guizal, *Phys. Rev. Lett.* **102**, 133901 (2009).
- <sup>18</sup>L. Peng, L. X. Ran, and N. A. Mortensen, *Appl. Phys. Lett.* **96**, 241108 (2010).
- <sup>19</sup>C. L. Holloway, E. F. Kuester, J. Baker-Jarvis, and P. Kabos, *IEEE Trans. Antennas Propag.* **51**, 2596 (2003).
- <sup>20</sup>O. G. Vendik and M. S. Gashinova, in Proceedings of the 34th European Microwave Conference (IEEE, Amsterdam, 2004), pp. 1209–1212.
- <sup>21</sup>Q. Zhao, L. Kang, B. Du, H. Zhao, Q. Xie, X. Huang, B. Li, J. Zhou, and L. Li, *Phys. Rev. Lett.* **101**, 027402 (2008).
- <sup>22</sup>Q. Zhao, L. Kang, B. Du, H. J. Zhao, Q. Xie, B. Li, J. Zhou, L. T. Li, and Y. G. Meng, *Chin. Sci. Bull.* **53**, 3272 (2008).
- <sup>23</sup>L. Lewin, *Proc. Inst. Electr. Eng.* **94**, 65 (1947).
- <sup>24</sup>J. C. Maxwell and B. A. Garnett, *Philos. Trans. R. Soc. London, Ser. A* **203**, 385 (1904).
- <sup>25</sup>V. Yannopapas and A. Moroz, *J. Phys. Condens. Matter* **17**, 3717 (2005).